

Measurement of Tagged Neutron Structure Functions using CLAS

A Letter of Intent to Jefferson Lab

Sebastian Kuhn*, Gail Dodge, Alexei Klimenko, Stepan Stepanyan, Lawrence Weinstein

Old Dominion University

Rolf Ent, Thia Keppel, Wally Melnitchouk, Will Brooks, Volker Burkert, Ioana Niculescu

Jefferson Lab

Keith Griffioen

The College of William and Mary

Marco Ripani, Marco Anghinolfi, Marco Battaglieri, Raffaella De Vita, Michail Osipenko,
G. Ricco, Silvano Simula, Mauro Taiuti

Istituto Nazionale di Fisica Nucleare, Genova, Italy

Misak Sargsian, Laird Kramer

Florida International University

Mark Strikman

Penn State University

John Arrington

Argonne National Lab

Gabriel Niculescu

Ohio University

Maurik Holtrop

University of New Hampshire

Franz Klein

Catholic University

Luminita Todor

Carnegie Mellon University

Sabine Jeschonnek

Ohio State University

David Gaskell

University of Colorado

* Contact: Sebastian Kuhn, Department of Physics, Old Dominion University, Norfolk VA 23529. Email: skuhn@odu.edu

1 Overview

Structure functions of the nucleon reflect the defining features of QCD: asymptotic freedom at large momenta and small distance scales, as well as confinement and non-perturbative effects at the hadronic scale. From measurements of these structure functions, one can infer the momentum and spin carried by the quarks and (via perturbative evolution) the gluons inside the nucleon. Via scaling violations and other higher-twist observables, one gains access to the quark-gluon dynamics in a bound hadronic system.

After more than three decades of measurements at many labs worldwide, an impressive amount of data has been collected, extending over several orders of magnitude in x (the fraction of the nucleon's momentum carried by the struck quark) and Q^2 (the squared 4-momentum transfer). However, there are still regions of the kinematic phase space where data are scarce or imprecise. Jefferson Lab can make an important contribution by filling these gaps with beam energies up to 6 GeV now, and up to 12 GeV in the future.

One of the most interesting open questions about the behavior of the structure functions is what happens at the extreme kinematic limit $x \rightarrow 1$, where nearly all of the nucleon momentum is carried by a single quark. This limit is dominated by the relative contributions of the u and d valence quarks. Simple phenomenological models like the SU(6) symmetric quark model predict significantly different behavior than perturbative QCD or quark models with improved hyperfine interactions. One can study this region via the ratio of the neutron and proton unpolarized structure functions F_2^n/F_2^p . Although F_2^p is well-known, F_2^n can only be deduced using nuclear targets which for inclusive experiments requires models for the nuclear physics and a subtraction of the F_2^p background.

Another interesting question is whether Bloom-Gilman duality holds as well for the neutron as it does for the proton. The beautiful data for F_2^p in the resonance region show remarkable agreement with extrapolations of the deep-inelastic results to lower Q^2 at comparable x , when one averages over the resonance peaks. No such precise comparison has yet been made for the neutron. Again, the main stumbling block is the absence of neutron data in the resonance region, where Fermi motion and off-shell effects wash out most of the resonance structures in inclusive electron scattering off a deuteron target. A better knowledge of neutron structure functions in the resonance region is also urgently needed to extract the full isospin structure of resonant and non-resonant contributions to the cross section, and to interpret polarized structure function measurements as well as nuclear structure functions in this kinematic domain.

In this Letter of Intent to the Jefferson Lab Program Advisory Committee, we describe a new experimental initiative to measure directly neutron structure functions at moderate to high x , via detection of a slow backward-going spectator proton. We propose to build a novel integrated target-recoil detector system for the CEBAF Large Acceptance Spectrometer (CLAS). This system will allow us to “tag” elastic and inelastic scattering on the neutron inside deuterium with a backward-going proton of less than 100 MeV/c momentum. While we concentrate here on deuterium as target and 4 - 6 GeV electron beams, there are many extensions (to higher and lower energy) and other experimental programs that could be undertaken with such a system.

In the following, we explain the theoretical motivation and experimental set up in more detail. We then sketch the planned target-detector system and the results of some very

preliminary simulations. We ask the PAC to comment both on the desirability and the feasibility of this experimental program. Following a positive recommendation by the PAC, we will develop a full proposal in the near future.

2 Theoretical background

Although a large body of structure function data exists over a wide range of x and Q^2 , the region $x > 0.6$ is not well-explored. For $x \geq 0.4$ the contributions from the $q\bar{q}$ sea are negligible, and the structure functions are dominated by the valence quarks.

Knowledge of the valence quark distributions of the nucleon at large x is vital for several reasons. The simplest SU(6) symmetric quark model predicts that the ratio of d to u quark distributions in the proton is $\frac{1}{2}$, however, the breaking of this symmetry in nature results in a much smaller ratio. Various mechanisms have been invoked to explain why the $d(x)$ distribution is softer than $u(x)$. For instance, if the interaction between quarks that are spectators to the deep inelastic collision is dominated by one-gluon exchange, then the d quark distribution will be suppressed and the d/u ratio tend to zero in the limit $x \rightarrow 1$ [1]. This assumption has been built into all global analyses of parton distribution functions [2], and must be independently tested. On the other hand, if the dominant reaction mechanism involves deep-inelastic scattering (DIS) from a quark with the same spin orientation as the nucleon, as predicted by perturbative QCD, then d/u tends to $\approx 1/5$ as $x \rightarrow 1$ [3]. Determining d/u experimentally would lead to important insights into the mechanisms responsible for spin-flavor symmetry breaking. In addition, quark distributions at large x are a crucial input for estimating backgrounds in searches for new physics beyond the Standard Model at high energy colliders [4].

Because of the 4:1 weighting of the squared quark charges, data on the proton structure function, F_2^p , provides strong constraints on the u quark distribution at large x ,

$$F_2^p(x) = x \sum_q e_q^2 (q(x) + \bar{q}(x)) \approx x \left(\frac{4}{9} u(x) + \frac{1}{9} d(x) \right). \quad (1)$$

The determination of the d quark distributions, on the other hand, requires in addition the measurement of the neutron structure function, F_2^n . In particular, d/u can be determined from the ratio

$$\frac{F_2^n}{F_2^p} \approx \frac{1 + 4d/u}{4 + d/u}, \quad (2)$$

provided $x \geq 0.4$ where sea quark contributions can be neglected.

Up to now, data on F_2^n have been extracted primarily from inclusive scattering off deuterium. Unfortunately, theoretical uncertainties in the treatment of nuclear corrections have led to ambiguities in the extracted F_2^n at large x . In particular, inclusion of Fermi motion and nucleon off-shell corrections in the deuteron can lead to values for F_2^n/F_2^p which differ by 50% already at $x = 0.75$ [5, 6]. The differences are even more dramatic if one extracts F_2^n on the basis of the nuclear density model [7]. The tagged structure function method for measuring F_2^n proposed here virtually eliminates the uncertainties from nuclear models.

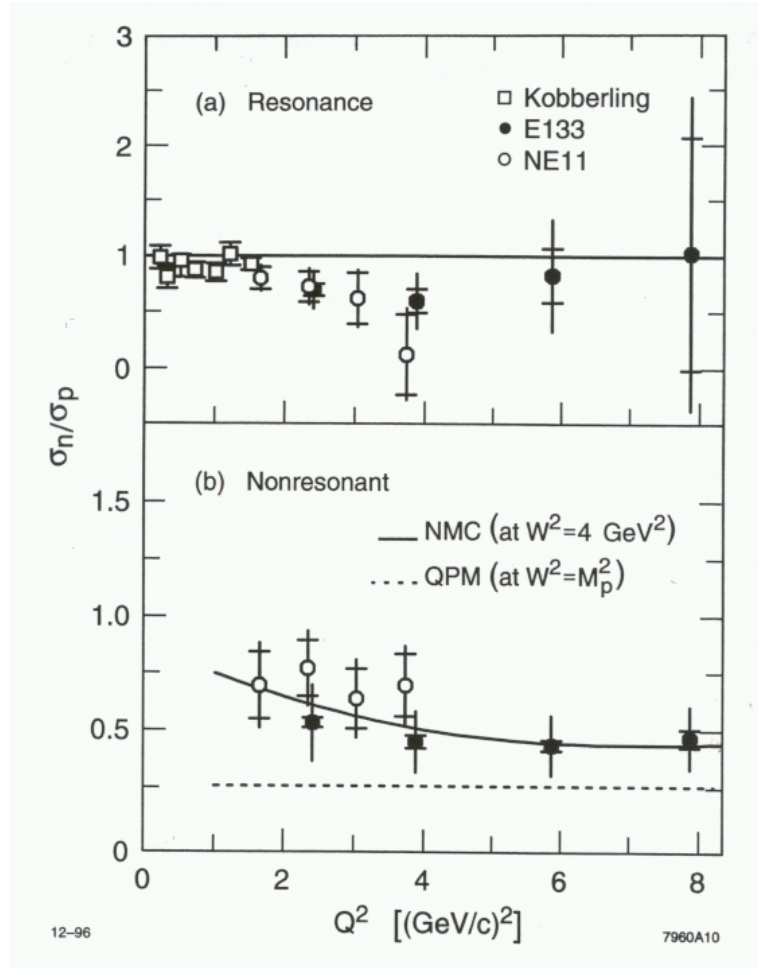


Figure 1: Extracted resonant and non-resonant contributions to the neutron to proton cross section ratio in the region of the Δ resonance[8].

Using a 6 GeV beam, we can make some initial measurements in the region of x where nuclear models begin to produce markedly different F_2^n/F_2^p values. However, a full exploration of the ratio F_2^n/F_2^p out to higher x will have to wait for the upgraded 11 GeV beam. We propose to focus also on the neutron resonance region which can be easily accessed kinematically at Jefferson Lab with present beam energies, and for which there are essentially no data. Measurements of resonance transition and elastic form factors provide fundamental information on the structure of the neutron and therefore are very interesting in their own right.

Figure 1 depicts the extracted resonant and non-resonant contributions to F_2^n/F_2^p for the $\Delta(1232)$ resonance as a function of Q^2 from 1 to 8 GeV² [8]. No other high Q^2 neutron resonance electroproduction data exist. The curves are from Refs. [9, 10]. An average over all Q^2 yields 0.72 ± 0.07 [8, 11] for σ_n/σ_p at the Δ resonance, whereas an average over low Q^2 data yields $\sigma_n/\sigma_p = 0.91 \pm 0.03$ [12]. It is interesting to note that the neutron- Δ transition form factor quite possibly exhibits the same anomalous behavior seen in the proton data [13, 14, 15, 16]. The largest uncertainty in extracting the neutron data depicted in Fig. 1 was the dependence of the assumed value of σ_n/σ_p for the S_{11} resonance, which is as yet unmeasured. A relativistic constituent quark model prediction for the $S_{11}(1535)$ resonance is approximately constant for $Q^2 > 1.5$ GeV² at $\sigma_n/\sigma_p = 0.3$ [17].

Measurements [18, 19] at JLab of the unpolarized structure functions on hydrogen in the resonance region have been used to verify Bloom-Gilman duality [20, 21]. With this, as well as polarized measurements, duality has been shown to be a fundamental property of nucleon structure. This work has inspired renewed theory interest in the topic (see for example [22]), and neutron data will add more valuable information. Specifically, Close and Isgur [23] argue that the neutron structure functions should exhibit “systematic deviations from local duality.” In their approach, minimal necessary conditions are identified for duality to occur in a simple harmonic oscillator quark model and these conditions occur at higher W for the neutron than for the proton. Understanding duality could prove to be crucial for mapping the transition from hadronic to quark-gluon degrees of freedom, and the measurements proposed here would allow one to identify the basic principles which underly this transition. Furthermore, if the systematics of Bloom-Gilman duality are understood quantitatively, duality could provide a powerful tool for accessing the large x region.

Although precision electron-proton scattering experiments have been performed in a straightforward manner with hydrogen targets, it has been necessary to infer experimental information on the structure of the neutron from nuclear (typically deuteron) data. The procedure of unfolding neutron data from inclusive nuclear cross sections, via the subtraction of Fermi motion effects and contributions from various nuclear constituents, leads to ambiguities dependent on the models and reaction mechanisms employed. This is particularly true for measurements at high x and moderate Q^2 (elastic and resonance regions).

To illustrate, consider the inclusive resonance electroproduction cross section spectra shown in Fig. 2. These data were obtained at Jefferson Lab at $Q^2 = 1.5$ GeV² for hydrogen and deuterium targets at matched kinematics. Although the three prominent resonance enhancements are obvious in the hydrogen data, only a hint of the first (the $\Delta(1232)$) is identifiable in the deuterium data. At $Q^2 > 2$ GeV², no discernable structure remains in the deuterium data. Neutron extraction from such data requires careful modeling of the resonant and non-resonant components for the neutron (as was done with the hydrogen

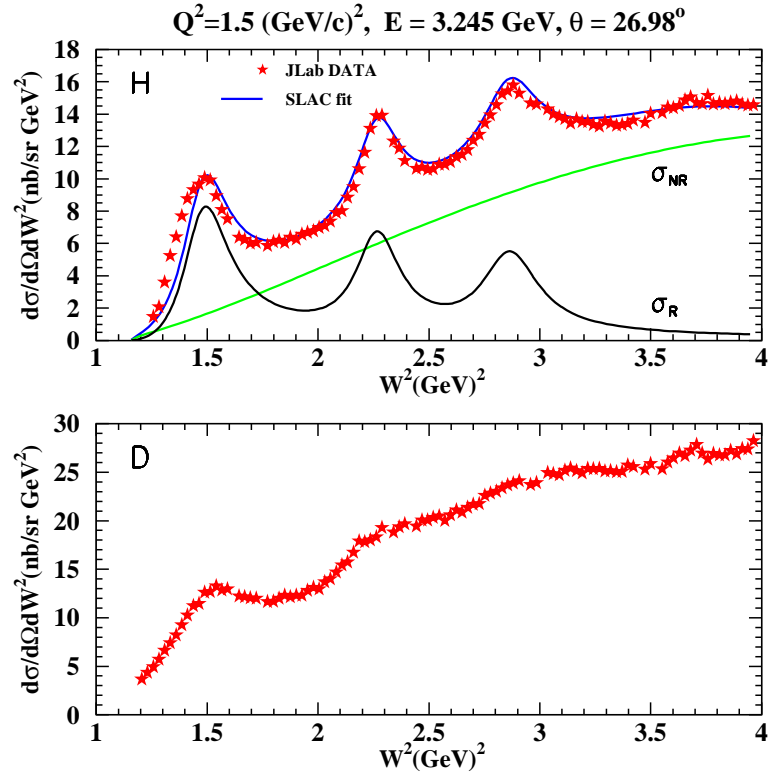


Figure 2: Inclusive resonance electroproduction cross sections from Jefferson Lab at $Q^2 = 1.5 \text{ GeV}^2$. Cross sections are shown as a function of invariant mass squared for hydrogen (top) deuterium (bottom) targets at matched kinematics. The hydrogen spectrum is plotted with global resonant and non-resonant fits.

data). Calculations must account for the nuclear effects of binding, Fermi motion, and nucleon off-shellness. The model-dependence introduced by each of these steps leads to a substantial uncertainty in the neutron resonance structure functions. For this reason very little neutron resonance transition form factor data exist.

The measurement of the tagged structure functions in semi-inclusive DIS from the deuteron with a slow recoil proton detected in the backward hemisphere, $e + D \rightarrow e + p + X$, may allow a resolution of the ambiguities introduced by nuclear model dependence both in the deep inelastic and the resonance region [24, 25, 26]. Within the nuclear impulse approximation, in which the deep inelastic scattering takes place incoherently from individual nucleons, the differential semi-inclusive cross section can be written as a product of the deuteron spectral function, \mathcal{S} , and an effective (bound) neutron structure function, $F_2^{n(eff)}$ [26]:

$$\frac{d\sigma}{dx dW^2 d\alpha_s d^2p_T} \approx \frac{2\alpha_{em}^2(1 - \nu/E)}{Q^4} \alpha_s \mathcal{S}(\alpha_s, p_T) F_2^{n(eff)}(W^2, Q^2, p^2). \quad (3)$$

Here $W^2 = (p_d + q - p_s)^2$ is the invariant mass squared of the unobserved hadronic final state, with p_s the momentum of the spectator proton, p_d the momentum of the initial state deuteron, and $p = p_d - p_s$ the momentum of the struck neutron. The variable $\alpha_s = (E_s - p_s^z)/M$ is the light-cone momentum fraction carried by the spectator proton and p_T its momentum component perpendicular to the direction of \vec{q} , with $E_s = \sqrt{M^2 + \vec{p}_s^2}$ the spectator proton energy and M its mass. In Eq.(3) the pre-factor α_s is related to the so-called “flux-factor” [27]. The degree to which the struck neutron is off-shell is given by

$$M^2 - p^2 \approx 2\vec{p}_s^2 + 2M\epsilon, \quad (4)$$

where ϵ is the deuteron binding energy. In the limit $p^2 \rightarrow M^2$, the effective neutron structure function $F_2^{n(eff)}(W^2, Q^2, p^2) \rightarrow F_2^n(W^2, Q^2, M^2) \equiv F_2^n(x, Q^2)$, the free neutron structure function. The p^2 dependence of $F_2^{n(eff)}$ depends strongly on the theoretical assumptions made about the off-shell behavior of the photon—bound-nucleon scattering amplitude. The ratio $R_n \equiv F_2^{n(eff)}(W^2, Q^2, p^2)/F_2^n(W^2, Q^2)$ of the bound to free neutron structure functions in the relativistic, covariant spectator model of Ref. [28] is shown in Fig. 3 for several values of x , as a function of the momentum of the spectator, $|\vec{p}_s| = |\vec{p}|$. Although the effect at low $|\vec{p}_s|$ is small, the deviation from unity increases sharply with increasing momentum, especially at larger values of x where the EMC effect is more pronounced. A similar behavior is observed in the non-relativistic model of Ref. [29], where the assumption of weak binding in the deuteron allows one to calculate the off-shell dependence up to order p^2/M^2 [29].

On the other hand, the color screening model for the suppression of point-like configurations (PLC) in bound nucleons [7], which attribute most or all of the EMC effect to a medium modification of the internal structure of the bound nucleon, predicts significantly larger (factor 2 or 3 [26]) deviations from unity than those in Fig. 3. It is important, therefore, that the tagged structure functions be measured for kinematics where the difference $p^2 - M^2$ is as small as possible, to minimize theoretical uncertainties associated with extrapolation to the nucleon pole. Since the deviation of the bound to free structure function ratio from the free limit is proportional to $2\vec{p}_s^2 + 2M\epsilon$ (Eq. (4)), sampling the data as a function of \vec{p}_s^2 should provide some guidance for a smooth extrapolation to the pole. In practice, considering momentum intervals of 100–200 MeV/c and 200–350 MeV/c would allow the

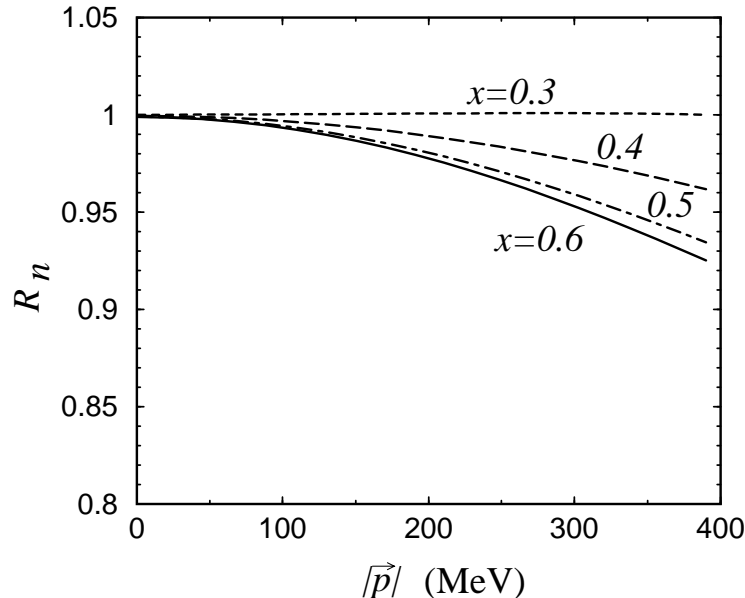


Figure 3: Ratio $R_n \equiv F_2^{n(eff)}(W^2, Q^2, p^2)/F_2^n(W^2, Q^2)$ of the bound to free neutron structure functions, as a function of the spectator proton momentum, in the model of Ref. [28].

dependence on p^2 to be constrained. The high-momentum kinematics (up to 700 MeV/c) will be well-measured by experiment E94-102 which ran in early 2002 in Hall B.

We expect only a few percent remaining uncertainty on the extrapolation to the on-shell point $p^2 = M^2$. This is also supported by recent $(\vec{e}, e'\vec{p})$ polarization transfer experiments at Mainz and Jefferson Lab on ^4He nuclei which indicate that the magnitude of the off-shell deformation may be rather small [30]. These experiments measured the ratio of transverse to longitudinal polarization of the ejected protons, which is related to the medium modification of the electric to magnetic elastic form factor ratio. Using model independent relations derived from quark-hadron duality, one can relate the small, but non-zero medium modification observed in the form factors to a modification at large x of the deep inelastic structure function of the bound nucleon [31], which suggests an effect of $\leq 3\%$ for $x \leq 0.8$. The typical momentum of the knocked out protons in the experiments was ~ 50 MeV, although the results of the analysis were found not to depend strongly on the proton momentum [31].

Another possible source of uncertainty lies in the final state interactions (FSI's)—the rescattering of the spectator proton by the deep-inelastic remnants, X , of the scattered neutron. Extraction of the free neutron structure function in this process is most reliable in the kinematic region where the FSI effects are small, and where different nuclear models for the deuteron spectral function, \mathcal{S} , lead to similar results. The choice of backward angles is designed to minimize these effects. Production of backward protons also suppresses contributions from direct processes, where a nucleon is produced in the γ^*N interaction vertex.

The magnitude of FSI effects has been estimated in Ref. [26] within the framework of the distorted wave impulse approximation (DWIA) [32]. Although a direct calculation of the FSI contribution to the cross section requires knowledge of the full dynamics of the spectator proton- X system, which is currently unavailable, one can estimate the uncertainty

introduced through neglect of FSI by comparing with the calculation of FSI effects in the high-energy $d(e, e'p)n$ break-up reaction [32]. The effective p - X interaction cross section, σ_{eff} , can be approximated [33] by that extracted from soft neutron production in the high-energy DIS of muons from heavy nuclei [34]. The effect of the FSI is to modify the spectral function $\mathcal{S} \rightarrow \mathcal{S}^{DWIA}$ [32], where

$$\mathcal{S}^{DWIA}(\alpha_s, p_T \approx 0) \sim \mathcal{S}(\alpha_s, p_T \approx 0) \left[1 - \frac{\sigma_{eff}(Q^2, x)}{8\pi \langle r_{pn}^2 \rangle} \frac{|\psi_D(\alpha_s, \langle p_T \rangle) \psi_D(\alpha_s, 0)|}{S(\alpha_s, p_T \approx 0) / \sqrt{E_s E_s(\langle p_T^2 \rangle)}} \right]. \quad (5)$$

Here $\langle r_{pn}^2 \rangle$ is the average separation of the nucleons within the deuteron, E_s is the spectator nucleon energy, and $E_s(\langle p_T^2 \rangle) = \sqrt{M^2 + p_z^2 + \langle p_T^2 \rangle}$ is the energy evaluated at the average transverse momentum $\langle p_T^2 \rangle^{1/2} \sim 200\text{--}300$ MeV/c transferred for the hadronic soft interactions with effective cross section σ_{eff} . The steep momentum dependence of the deuteron wave function, $|\psi_D(\alpha_s, \langle p_T \rangle)| \ll |\psi_D(\alpha_s, p_T \approx 0)|$, ensures that FSI effects are suppressed in the extreme backward kinematics.

The effects of FSI are illustrated in Fig.4, which shows the ratio of the light-cone spectral function including FSI effects within the DWIA to that without [26]. At extreme backward kinematics ($p_T \approx 0$) one sees that FSI effects contribute less than $\sim 5\%$ to the overall uncertainty of the $d(e, e'n)X$ cross section for $\alpha_s \leq 1.5$. This number can be considered as an upper limit on the uncertainties due to FSI. At larger p_T (≥ 0.3 GeV/c), and small α_s (≈ 1), the double scattering contribution (which is not present for the extreme backward case, see Eq. 5) plays a more important role in FSI [32].

Another potential correction to Eq. 3 is from the breaking of the factorization approximation. In the inclusive structure function analysis in Ref. [28] these were found to be small ($\leq 1\%$) for the range of x considered here. To further minimize possible theoretical ambiguities one should restrict the analysis to spectator momenta below $\approx 150\text{--}200$ MeV/c.

Of course, in order to identify any residual nuclear effects, it would be ideal to repeat this experiment by detecting spectator neutrons. Comparing the bound proton structure function with the free proton structure function would then allow one to correct the bound neutron structure function for any remaining nuclear effects. However, building a neutron detector for this purpose is extremely challenging technically because of the large electromagnetic backgrounds present.

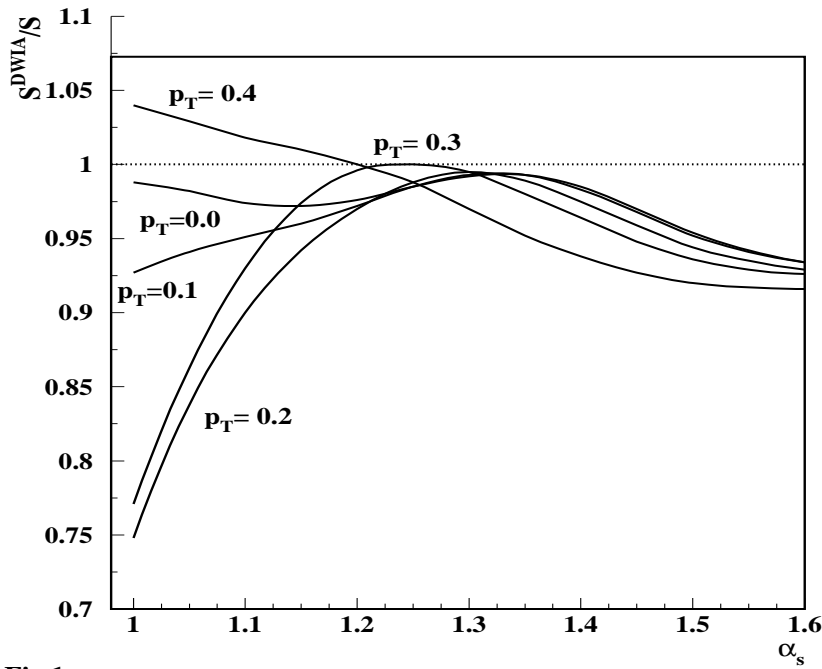


Fig.1

Figure 4: Spectral function calculated with and without FSI effects within the DWIA [26]. The curves correspond to different values of the spectator nucleon transverse momentum (in GeV/c).

3 Recoil detector

Improvements in the rate capability of vertex detectors over the last decade, driven by the needs of the high-energy physics community, enables us to use a new tagging technique for relatively low-energy charged recoil particles. We propose to build a 30 cm long, 20 cm diameter, 5 atm target-detector gas vessel. The inner 10 cm diameter will contain 5 atm deuterium gas that will act as the target in the CLAS detector. The surrounding cylindrical detector consists of six layers of Gas Electron Multiplier (GEM)/microstrip detectors, a technology developed by Fabio Sauli at CERN. This detector will operate at a pressure of 5 atm argon gas. A thin aluminized mylar foil is used to separate the 5 atm deuterium gas from the 5 atm argon gas, while an additional gas vessel will be used to permanently maintain zero differential gas pressure. In this case, a beam current of 100 nA yields a luminosity of 5×10^{33} electron-atoms/cm²/s. The deuterium target gas can easily be replaced by another target gas such as helium, argon or xenon.

The GEM is a perforated foil of insulating material coated on both sides with a thin metal layer. The GEM is used as an internal charge preamplification device [35], to overcome the problems encountered when using Micro Strip Gas Chambers (MSGC). With suitable potential applied, the GEM acts as powerful preamplifier for electrons released by ionizing radiation in a gas, transferring most of the multiplied electron charge to a pickup electrode or to another amplifying device. Several studies to determine the GEM's sensitivity to soft X-rays and charged particles have been made both in the test laboratory and with beam conditions [36, 37, 38, 39, 40, 41, 42, 43, 44, 45].

In the proposed detector (see Fig. 5), each GEM detector has the same standard structure. Primary ionization is produced by radiation in a first drift region, amplified by the GEM. A second, induction, region is used to collect the amplified electrons by readout boards. Both

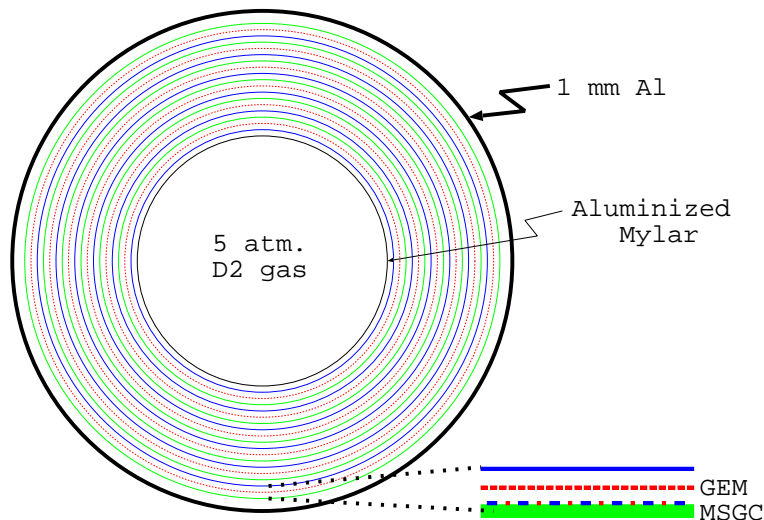


Figure 5: Schematic drawing of the proposed target-recoil detector system. The target volume (5 atm deuterium gas) is surrounded by 6 layers of GEM detectors operated with 5 atm Argon gas and read out with microstrip readouts.

drift and induction gas regions are a few millimeters thick, and filled with Argon gas. The GEM sheet consists of 50 μm thin insulation foil, with 5 μm copper cladding on both sides. The thicknesses and materials we intend to use for this composite detector are all relatively standard, however we are at the limits of the technology in timing performance. Decent timing (<10 ns) is required to provide a real to accidental ratio of better than unity in the tagging process. The outer area of the 5 atm detector will consist of one mm of Al to provide a safety factor of at least four, assuming that we might want to operate at a 10 atm pressure at a later date. The construction of this high-pressure cylindrical GEM detector is the main research and development project necessary for the proposed program.

Realistic simulations indicate the possibility to detect spectator protons with momenta between 70 and 200 MeV/c with this composite detector. The resolution in momentum obtained is less than 7 MeV/c (rms). The minimum necessary gain for a 5 atm Argon detector is ≤ 20 , whereas gains of over 100 at 7 atm operating pressure have been shown in the laboratory [46]. This minimum necessary gain prescribes how many electrons need to be collected during an integration time to minimize electronic noise related to modern high-density fast electronics.

In order to suppress possible contaminations from spectator protons boosted in momentum by slow pions associated with the deep inelastic process, we intend to initially use only protons in the backward hemisphere with respect to the momentum transfer [47]. Calculations and analysis of older neutrino data show that this should suppress these reaction mechanism effects sufficiently [48].

Most of the background in the proximity of the production target is due to Möller scattering of electrons from the atomic electrons in the deuterium gas. During standard CLAS operation this background is kept away from the Region 1 drift chamber by a normal conducting toroidal magnet, called the “mini-torus”. However, improved shielding is obtained using a longitudinal magnetic field, as demonstrated by the 5 Tesla polarized target magnet

in the eg1 experiment. This arrangement decreases the Moller backgrounds by a factor of 2.

The E1-DVCS collaboration (E-01-113) is currently designing a superconducting solenoid arrangement that will serve the same purpose. However, the advantage over the eg1 target magnet is that the magnet cryostat will have a warm bore, allowing easy access to the target region, as required by the proposed experiment. The requirements for the DVCS experiment are very close to what is needed for what is proposed in this LOI. The current magnet design uses an approximately 5 Tesla central magnetic field to guide the low-energy Möller electrons sufficiently far away from the target area where they can be dumped in a heavy metal shielding pipe. The construction of the DVCS magnet is scheduled to be completed by the end of the year 2003.

One of the biggest demands on the design of the experiment proposed here is the suppression of accidental (e,p) coincidences. Experimental information on the cross sections for detection of low-momentum hadrons is only sparse. Most of the existing experimental information is based upon experiments where target materials and/or windows prevented the detection of low-momentum particles. Furthermore, due to rate constraints, most electron scattering experiments have concentrated on the forward hemisphere of detection. Therefore, the calculation of singles rates that will be encountered with the proposed setup is non-trivial. Assuming a luminosity of 5×10^{33} electron-atoms/cm²/s, EPC would predict a total rate of about 3 MHz in the full detector, for protons with momenta larger than 50 MeV/c. However, experimental information, e.g. in Hall C tests, indicates that (e,p) rates are typically far lower than the EPC predictions for low-momentum protons in the backward hemisphere. The Hall C tests showed a reduction of at least one order of magnitude with respect to the EPC calculation for protons between 100 and 200 MeV/c originating at an angle of 90°.

A simple calculation, assuming that the recoil detector will see the total rate from the deuteron photodisintegration process, would give an upper limit of 10 MHz (e,p) singles.

Obviously, the total rate should not be a critical issue for the proposed, highly segmented, GEM detector setup. However, the (e,p) singles rate is relevant for the spectator tagging process we propose. The spectator tagging efficiency will always be smaller than unity, as we only detect spectator protons with momenta between 70 and 200 MeV/c. This constitutes only about 50% of the full deuteron wave function integral. In addition, the detector will not cover the full phase space. Thus, in practice, one will measure only a certain fraction of (e,e') events in coincidence with a spectator proton. In this situation the real to accidental ratio is directly proportional to the (inverse of) the (e,p) hadron singles rates. Assuming a timing window of 10 ns, the real to accidental ratio would be better than 3:1, assuming the EPC predictions. This ratio can be further improved by using vertex reconstruction.

4 Expected results

For the first full proposal we plan to submit, we will probably focus on data in the resonance region and at moderately high x , requiring running at two beam energies, e.g., 4 GeV and 6 GeV. For illustrative purpose, here we have simulated the expected results from a 40 day (100% efficient) run at 6 GeV in CLAS with the recoil detector as described above. We require a minimum momentum of 70 MeV/c for proper detection of a proton going perpendicular to

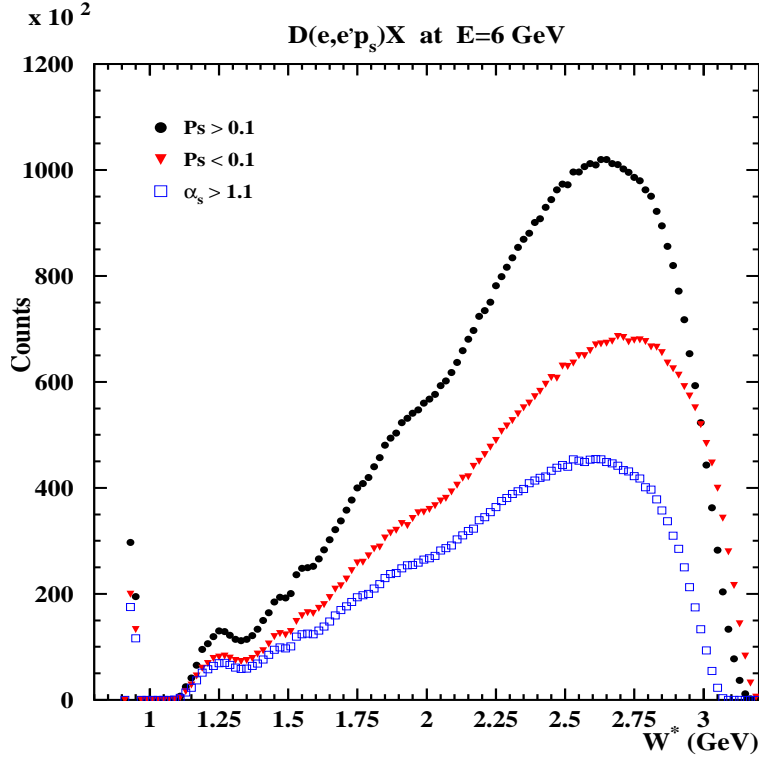


Figure 6: Expected number of counts for the proposed experiment in 40 days of ideal running at 6 GeV, plotted as a function of the reconstructed mass W of the (unobserved) final state. The data sets are for different cuts on the momentum p_s and the light cone fraction α_s of the spectator. Clearly, there will be ample statistics to study F_2^n in the resonance region and beyond, and to further subdivide the accessible range $1 \text{ GeV}^2 < Q^2 < 5 \text{ GeV}^2$ into several bins in Q^2 .

the detector axis, and accordingly more (due to energy loss) for protons at different angles. We used a simple model of the acceptance of both CLAS for the scattered electrons and of the recoil detector for protons. To select events where the neutron is nearly on-shell, we require that the recoil momentum is less than 180 MeV/c ($M^2 - p^2 < 0.07 \text{ GeV}^2$). We also require that the spectator makes an angle of at least 110° with the momentum transfer vector \mathbf{q} .

Under these conditions, we expect nearly 10 M coincident events total, and 4 M events with recoil momentum below 100 MeV/c. The average spectator light cone fraction will be $\alpha_s = 1.08$. We will cover a range in W from the elastic peak to about $W = 3.2 \text{ GeV}$.

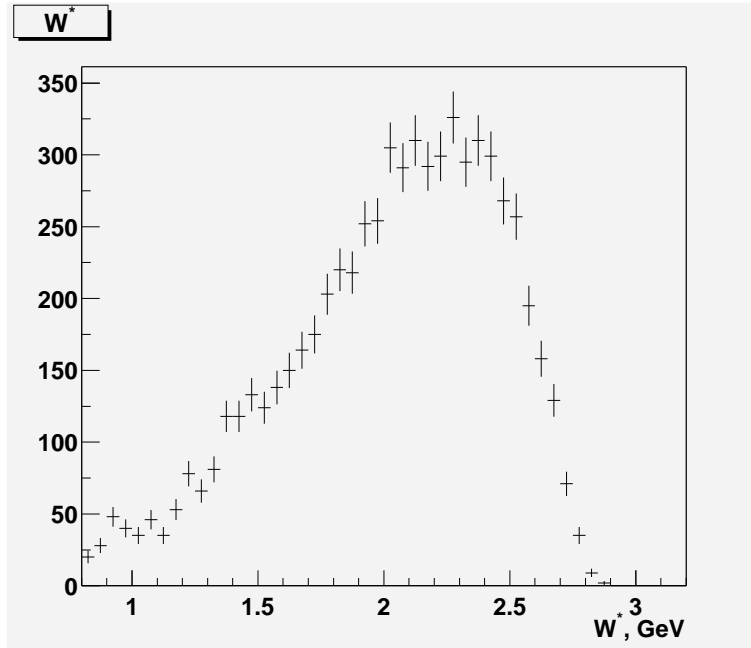


Figure 7: Preliminary spectrum from the recently completed e6 run at CLAS (counts versus reconstructed final state mass W), based on about 1% of the e6 data (5 hours). Similar cuts as proposed here were applied, but the threshold for detection of the recoil proton was above 200 MeV/c for this experiment. The resolution is expected to improve significantly once final calibrations and momentum corrections have been applied.

In Fig. 6, we show the expected number of coincident events of the type $d(e,e'p_s)X$, with the spectator going backwards with respect to \mathbf{q} , as a function of the reconstructed mass W of the unobserved final state. An example of this reconstruction is shown in Fig. 7, which is based on 1% of the existing data from CLAS experiment E94-102 (E6). This experiment covers the recoil momentum range above the limit proposed here (250 MeV/c). Comparison of the two data sets will allow us to study and correct for off-shell effects which will be much stronger for the e6 data.

Turning to the region $W > 1.8 \text{ GeV}$ (where resonant final states have little influence), we will collect data for $0.1 < x < 0.7$, with sufficient statistics to bin in several values of Q^2 from 1 to 5 GeV^2 and to study the dependence on the recoil momentum. As an example we show in Fig. 8 the statistical precision we can achieve for the ratio F_2^n/F_2^p as a function of x ,

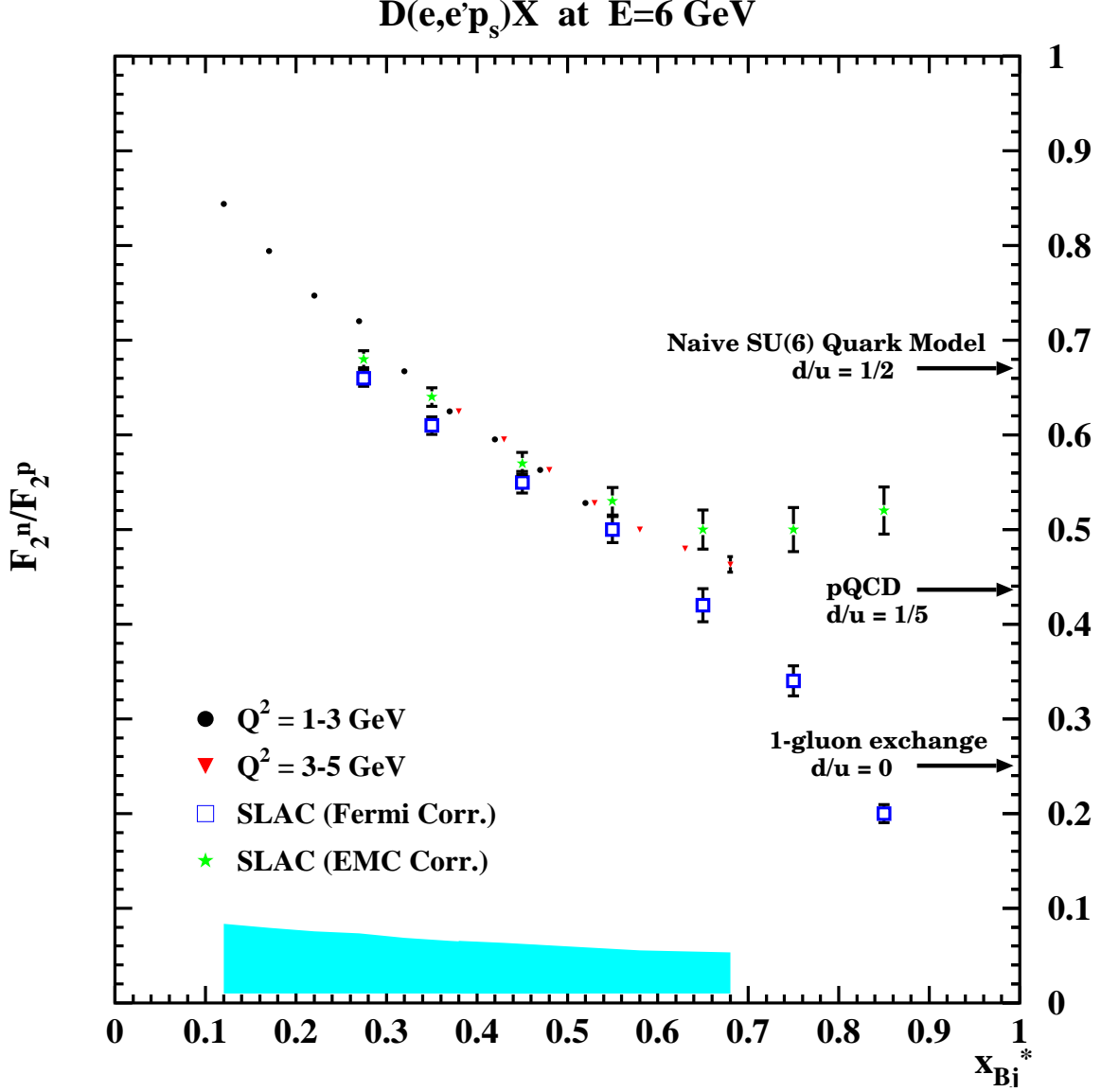


Figure 8: Ratio F_2^n/F_2^p versus x . The circles and triangles indicate the expected coverage of the proposed experiment for two different bins in Q^2 . The statistical error bars (smaller than the symbols for most points) are based on a 40 day run, with full reconstruction of the kinematics via detection of a backwards moving spectator proton. Estimated systematic errors due to experimental and theoretical uncertainties are indicated by the band at the bottom. The arrows indicate different possible approaches to the limit $x \rightarrow 1$ which cannot be excluded by present-day data due to the uncertainty of nuclear effects. The remaining points indicate existing (deuterium and proton) data from SLAC (with systematic and statistical error bars combined), analyzed in two different ways. In one case (open squares), the data on deuterium were only corrected for momentum smearing (Fermi correction). In the other case (stars), a parametrization of the EMC effect was used to correct the data.

for two different bins in Q^2 . The shaded band on the x -axis indicates a preliminary estimate of the total systematic error, from the combined experimental (acceptance, efficiency, event reconstruction, luminosity) and theoretical (deuteron wave function, off-shell and final state interaction effects) uncertainties. Note that many of these systematic uncertainties are uniform over the full range of x (for instance the probability of finding a spectator proton with certain kinematics in deuterium), so that the uncertainty on the slope of the ratio F_2^n/F_2^p will be much smaller. By normalizing our data to the well-known (and theoretically unproblematic) data at low x , we can extract the high- x behavior with much smaller uncertainty. Clearly, the data set indicated in Fig. 8 will improve considerably on the existing statistical uncertainty in the region of high x and at the same time distinguish between different interpretations of the existing data based on different models of nuclear effects.

5 Summary

We propose the construction of a gas target with Gas Electron Multiplier (GEM) microstrip detectors for measuring recoiling protons or light nuclei in CLAS. Such a detector paves the way for a new class of experiments on atomic nuclei at Jefferson Lab. By tagging the electron scattering from a nucleon with the nuclear remnants, we can measure the nucleon's motion before scattering and control how far off shell it was. This is especially important at high x where Fermi-motion effects in inclusive measurements are substantial. Essential for such measurements is the experimental requirement to observe the smallest possible recoil momenta for the nuclear remnants. With the proposed GEM detector, this limit is around 70 MeV/c for protons.

In the case of deuterium, a low-momentum recoiling proton insures that off-shell effects on the neutron are small and we can accurately correct the kinematics for a moving neutron. In the present letter of intent we concentrate on high- x neutron structure functions in deuterium. We wish to measure the resonance and deep-inelastic F_2^n structure function of the neutron for 6 GeV and 4 GeV electron beams in CLAS. This provides crucial data as high as $x = 0.7$ for the ratio F_2^n/F_2^p . This measurement can be extended to 11 GeV which would provide coverage up to $x = 0.85$.

At the same time, we can study the evolution of the neutron resonances. Unlike for a proton target, neutron resonances are blurred considerably by Fermi motion. The tagging process will restore the resonance widths to their intrinsic values, and facilitate a better analysis of resonance strength distributed over the range $1 < W < 2$ GeV.

Part of this proposal tests duality for the neutron. Insofar as duality holds for the nucleon resonance region, the F_2^n/F_2^p ratios can be extended to even higher values of x .

These experiments with the GEM detector nicely complement those of the e6 run period in which recoil protons were detected in CLAS for reactions on deuterium. In this case, the minimum proton momentum was about 200 MeV/c. Thus, there is already experience and data for high recoil momenta.

The GEM detector provides an unusual opportunity to study any exclusive reaction on the neutron that heretofore was clouded by uncertainty of whether a neutron or proton was struck in the reaction, or by Fermi motion.

Since the GEM detector can use any of a number of gases as target material, one can

envision future experiments with ^3He , ^4He , Ar, Xe, etc. For example, for an accurate determination of F_2^n/F_2^p , one could use a ^4He target, alternately tagging on ^3He recoils (a struck neutron) and ^3H recoils (a struck proton), thus forming the ratio in a single experiment with small systematic errors. Since both recoiling nuclei are charged, they are both detectable in the GEM.

The GEM is appropriate for low- t coherent vector meson production experiments, in which the nucleus in question must remain in its ground state. It can also be used to measure the decay products of a large nucleus that is highly excited following deep-inelastic scattering, since at JLab energies the struck quark should begin to hadronize within the nuclear volume. Other possible applications include scattering of a virtual "cloud" pion tagged by a backward proton, with hydrogen as target.

This rich program is improved and extended by higher beam energies. Therefore, measurements now at 6 GeV provide a tantalizing view of what is possible with the 11 GeV upgrade.

References

- [1] R.P. Feynman, *Photon Hadron Interactions* (Benjamin, Reading, Massachusetts, 1972); F.E. Close, Phys. Lett. **B43**, 422 (1973); Nucl. Phys. **B80**, 269 (1973); R.D. Carlitz, Phys. Lett. **B58**, 345 (1975); N. Isgur, Phys. Rev. D **59**, 034013 (1999).
- [2] A.D. Martin, R.G. Roberts, W.J. Stirling and R.S. Thorne, Eur. Phys. J. C **14**, 133 (2000); H.L. Lai *et al.*, Eur. Phys. J. C **12**, 375 (2000); M. Glück, E. Reya and A. Vogt, Eur. Phys. J. C **5**, 461 (1998).
- [3] G.R. Farrar and D.R. Jackson, Phys. Rev. Lett. **35**, 1416 (1975).
- [4] S. Kuhlmann *et al.*, Phys. Lett. **B476**, 291 (2000).
- [5] L.W. Whitlow *et al.*, Phys. Lett. **B282**, 475 (1992); A. Bodek, S. Dasu and S. E. Rock, in Tucson Part. Nucl. Phys., 768 (1991), SLAC-PUB-5598.
- [6] W. Melnitchouk and A.W. Thomas, Phys. Lett. **B377**, 11 (1996).
- [7] L. L. Frankfurt and M. I. Strikman, Nucl. Phys. **B250**, 1585 (1985); Phys. Rep. **160**, 235 (1988).
- [8] L. Stuart *et al.*, SLAC-PUB-6305 (1996), Phys. Rev. D **58**, 032003 (1998).
- [9] L.W. Whitlow *et al.*, Phys. Lett. **B282**, 475 (1992).
- [10] P. Amaudruz *et al.*, Phys. Lett. **B295**, 159 (1992).
- [11] S. Rock *et al.*, Phys. Rev. D **46**, 24 (1992).
- [12] M. Kobberling *et al.*, Nucl. Phys. **B82**, 201 (1974).
- [13] P. Stoler, Phys. Reports **226**, 103 (1993).

- [14] P. Stoler, Phys. Rev. Lett. **66**, 1003 (1991).
- [15] P. Stoler, Phys. Rev. D **44**, 73 (1991).
- [16] C. Keppel, Proceedings of the Workshop on CEBAF at Higher Energies, eds. N. Isgur and P. Stoler (April 1994) 237.
- [17] M. Warns *et al.*, Phys. Rev. D **42**, 2215 (1990).
- [18] I. Niculescu, *et al.*, Phys. Rev. Lett. **85**, 1186 (2000); I. Niculescu, *et al.*, Phys. Rev. Lett. **85**, 1182 (2000); R. Ent, C.E. Keppel, and I. Niculescu, Phys. Rev. D **62**, 073008 (2000); S. Liuti, R. Ent, C.E. Keppel and I. Niculescu, hep-ph/0111063.
- [19] M.E. Christy *et al.*, E94110 Collaboration, in preparation.
- [20] E.D. Bloom and F.J. Gilman, Phys. Rev. D **4**, 2901 (1970).
- [21] A. De Rujula, H. Georgi and H.D. Politzer, Ann. Phys. **103**, 315 (1977); H. Georgi and H.D. Politzer, Phys. Rev. D **14**, 1829 (1976).
- [22] V.V. Davidovsky and B.V. Struminsky, hep-ph/0205130; S. Jeschonnek and J.W. Van Orden, Phys. Rev. D **65**, 094038 (2002); and N. Isgur, S. Jeschonnek, W. Melnitchouk and J.W. Van Orden, Phys. Rev. D **65**, 054005 (2001).
- [23] F.E. Close and N. Isgur, Phys. Lett. B **509**, 81 (2001).
- [24] L. L Frankfurt and M. I. Strikman, Phys. Rep. **76**, 217 (1981).
- [25] S. Simula, Phys. Lett. **B387**, 245 (1996).
- [26] W. Melnitchouk, M. Sargsian and M.I. Strikman, Z. Phys. **A359**, 99 (1997).
- [27] See e.g. R.P. Bickerstaff and A.W. Thomas, J. Phys. G **15**, 1523 (1989).
- [28] W. Melnitchouk, A.W. Schreiber and A.W. Thomas, Phys. Lett. **B335**, 11 (1994); Phys. Rev. D **49**, 1183 (1994).
- [29] S. A. Kulagin, G. Piller and W. Weise, Phys. Rev. C **50**, 1154 (1994); S. A. Kulagin, W. Melnitchouk, G. Piller and W. Weise, Phys. Rev. C **52**, 932 (1995).
- [30] S. Dieterich *et al.*, Phys. Lett. **B500**, 47 (2001); R. Ransome, Nucl. Phys. **A699**, 360 (2002).
- [31] W. Melnitchouk, K. Tsushima, A.W. Thomas, Eur. Phys. J. A **14** (2002), nucl-th/0110071.
- [32] L. L. Frankfurt *et al.*, Z. Phys. **A352**, 97 (1995); Phys. Lett. **B369**, 201 (1996).
- [33] M. I. Strikman, M. Tverskoy, and M. Zhalov, in Proceedings of Workshop “Future Physics at HERA”, Hamburg, pp.1085-1088 (1996), nucl-th/9609055.

- [34] M. R. Adams *et al.*, Phys. Rev. Lett. **74**, 5198 (1995).
- [35] F. Sauli, Nucl. Instr. and Meth. **A386**, 531 (1997).
- [36] R. Bouclier, M. Capeans, W. Dominik, M. Hoch, J.-C. Labbe, G. Million, L. Ropelewski, F. Sauli, A. Sharma, IEEE Trans. Nucl. Sci. NS-44, 646 (1997).
- [37] R. Bouclier, W. Dominik, M. Houch, J.-C. Labbe, G. Million, L. Ropelewski, F. Sauli, A. Sharma, G. Manzin, Nucl. Instr. and Meth. **A396**, 50 (1997).
- [38] J. Benlloch, A. Bressan, M. Capeans, M. Gruwe, M. Hoch, J.-C. Labbe, A. Placci, L. Ropelewski, F. Sauli, Nucl. Instr. and Meth. **A419**, 410 (1998).
- [39] J. Benlloch, A. Bressan, C. Buttner, M. Capeans, M. Gruwe, M. Hoch, J.-C. Labbe, A. Placci, L. Ropelewski, F. Sauli, A. Sharma, R. Veenhof, IEEE Trans. Nucl. Sci. NS-45, 234 (1998).
- [40] C. Buttner, M. Capeans, W. Dominik, M. Hoch, J.-C. Labbe, G. Manzin, G. Million, L. Ropelewski, F. Sauli, A. Sharma, Nucl. Instr. and Meth. **A409**, 79 (1998).
- [41] W. Beaumont, T. Beckers, J. DeTroy, V. Van Dyck, O. Bouhali, F. Udo, C. VanderVelde, W. Van Doninck, P. Vanlaer, V. Zhukov, Nucl. Instr. and Meth. **A419**, 394 (1998).
- [42] R. Bellazzini, A. brez, G. Gariano, L. Latronic, N. Lumb, G. Spandre, M.M. Massai, R. Raffo, M.A. Spezziga, Nucl. Instr. and Meth. **A419**, 429 (1998).
- [43] A. Bressan, J.-C. Labbe, P. Pagano, L. Ropelewski, F. Sauli, Nucl. Instr. and Meth. **A425**, 254 (1999).
- [44] A. Bressan, L. Ropelewski, F. Sauli, D. Mormann, T. Muller, H.J. Simonis, Nucl. Instr. and Meth. **A425**, 262 (1999).
- [45] S. Bachmann, A. Bressan, L. Ropelewski, F. Sauli, A. Sharma, D. Mormann, Nucl. Instr. and Meth. **A438**, 376 (1999).
- [46] F. Sauli, private communications.
- [47] S. Simula, unpublished (2002).
- [48] G.D. Bosveld, A.E.L. Dieperink, and A.G. Tenner, Phys. Rev. C **49**, 2379 (1994).